Appl Phys B (2011) 104:145–149
DOI 10.1007/s00340-011-4456-9

Applied Physics B
Lasers and Optics

Enhanced performances of Yb^{3+}:$YAl_3(BO_3)_4$ laser crystal grown in Li_2WO_4–B_2O_3 flux

Y.J. Chen · N. Ye · Y.F. Lin · Z.D. Luo · Y.D. Huang

Received: 26 September 2010 / Revised version: 30 January 2011 / Published online: 3 June 2011

Abstract Yb^{3+}:$YAl_3(BO_3)_4$ crystals were grown in Li_2WO_4–B_2O_3 and $K_2Mo_3O_{10}$–B_2O_3 fluxes, respectively. In the same experimental conditions, a shorter ultraviolet absorption edge of 278 nm, longer fluorescence lifetime of 1.1 ms, higher slope efficiency of 58%, and lower threshold of 2.4 W were obtained in a Yb^{3+}:$YAl_3(BO_3)_4$ crystal grown in Li_2WO_4–B_2O_3 flux, whereas the corresponding values for the crystal grown in $K_2Mo_3O_{10}$–B_2O_3 traditional flux were 318 nm, 0.7 ms, 46%, and 3.1 W, respectively. Therefore, spectroscopic and laser performances of the one grown in Li_2WO_4–B_2O_3 flux are enhanced due to the improved crystal optical quality.

1 Introduction

Yb^{3+}:$YAl_3(BO_3)_4$ (Yb:YAB) crystal has been demonstrated as an excellent gain medium for microchip and self-frequency-doubling (SFD) green lasers in the past decade, because it possesses large nonlinear optical coefficient, good mechanical strength, high thermal conductivity, stable chemical characteristics, and good spectroscopic properties [1–4]. Maximum output power of 10.6 W at 1042 nm has been obtained by Liu et al. [4]. Continuous-wave (CW) green laser with 1.1 W output power and acousto-optic Q-switching pulse green laser with 2.27 W average output power have also been realized by SFD in diode-pumped Yb:YAB crystals [5, 6]. Due to the high fluorescence quantum efficiency of the $^2F_{5/2}$ multiplet and low quantum defect of Yb^{3+} ions, the slope efficiency obtained in Yb^{3+} lasers may be close to its theoretical limit of about 90% when the design of laser cavity and thermal arrangement of gain medium have been optimized [7, 8]. However, the highest slope efficiency obtained in Yb:YAB laser is only 72% presently [4]. The optical quality of Yb:YAB crystal may be one of the main limited factors for obtaining higher efficiency.

Because of its incongruent melting, YAB crystals can only be grown by flux method and various solvent systems have been investigated as a flux for the crystal growth [9]. Among them, $K_2Mo_3O_{10}$–B_2O_3 solvent system has been considered as the most suitable flux and widely used in the growth of YAB crystal at present [1, 9–12]. However, this complex polymolybdate flux has relatively high volatility. The volatilization of the solvent will change the composition and then the saturation temperature of the solution in growth process, which leads the instability during crystal growth. Moreover, a large amount of the foreign Mo impurity in the solvent may be incorporated into the crystal [9, 10]. Therefore, many defects, such as twinning, dislocation, and impurity, exist in YAB crystal grown in the complex polymolybdate flux and debase the crystal optical quality [12, 13]. In this work, Yb:YAB crystal with higher optical quality is successfully grown in Li_2WO_4–B_2O_3 solvent system, which has lower volatility at high temperature and higher dissolving ability in comparison with the conventional polymolybdate flux. The lower volatility can lead to a more stable growth condition. Furthermore, spectroscopic and laser performances of the Yb:YAB crystal are compared with those grown in $K_2Mo_3O_{10}$–B_2O_3 flux.

Y.J. Chen · N. Ye · Y.F. Lin · Z.D. Luo · Y.D. Huang (✉)
Key Laboratory of Optoelectronic Materials Chemistry and Physics, Fujian Institute of Research on the Structure of Matter, Chinese Academy of Sciences, Fuzhou, Fujian 350002, China
e-mail: huyd@fjirsm.ac.cn
Fax: +86-591-83715544

2 Growth of Yb:YAB crystal in Li_2WO_4–B_2O_3 flux

Yb:YAB crystals were grown in Li_2WO_4–B_2O_3 and $K_2Mo_3O_{10}$–B_2O_3 fluxes, respectively. For the crystal growth in Li_2WO_4–B_2O_3 flux, the composition of the mixture was 2(Yb:YAB):$3Li_2WO_4$:$5B_2O_3$ (mol%), which is the optimal one with suitable crystallization temperature and acceptable viscosity. The starting materials used were powders of Yb_2O_3 and Y_2O_3 with 99.99% purity, Al_2O_3, H_3BO_3, Li_2CO_3, and WO_3 with analar grade. All the powders were mixed and heated in a platinum crucible with a diameter of 60 mm and a height of 60 mm to 1100°C. This temperature was held for two days to ensure complete melting and homogeneity of the melt. A seed with orientation [100] was used to determine the crystallization temperature and initiate growth. A crystal was grown by cooling at a rate of 1–2°C/day until a desired boule size was obtained. Then the crystal was pulled out of the melt and cooled down together with the furnace to room temperature at a rate of −20°C/h. The flux attached to the crystal can be easily dissolved in hot nitric acid solution. The detailed crystal growth process with $K_2Mo_3O_{10}$–B_2O_3 flux can be found in the previous reports [1, 9–11].

Yb^{3+} concentrations in the crystals were measured by inductively coupled plasma atomic emission spectrometry (ICP-AES, Ultima 2, Jobin-Yvon) and both of them were about 10 at.% (5.5×10^{20} cm^{-3}). The sizes of the grown Yb:YAB single crystals in Li_2WO_4–B_2O_3 and $K_2Mo_3O_{10}$–B_2O_3 fluxes were both close to $30 \times 25 \times 20$ mm^3. Both crystals were transparent. However, the former was colorless and the latter had a faint yellowish tinge, which has also been observed in Ref. [1]. Both crystals were *c*-cut and then polished to be 1.0-mm thick for spectroscopic and laser experiments.

The volatilities of both solvent systems were measured by keeping the melts at 1100°C for 290 h in a platinum crucible with a diameter of 30 mm and a height of 30 mm, and are shown in Fig. 1. The compositions of the melts are the same as those used in crystal growth experiments. The mass losses of the melts were recorded at an interval of 10–30 h. The initial total amount of each melt was 10 g. It can be seen from the figure that the volatility of Li_2WO_4–B_2O_3 flux is far lower than that of $K_2Mo_3O_{10}$–B_2O_3 flux. The volatility of $K_2Mo_3O_{10}$–B_2O_3 flux increases quickly with the melting hour whereas that of Li_2WO_4–B_2O_3 flux changes slightly. Due to the long period needed for the growth of YAB crystal, above characteristic of Li_2WO_4–B_2O_3 flux can ensure the stability of the crystal growth and then the higher crystal optical quality.

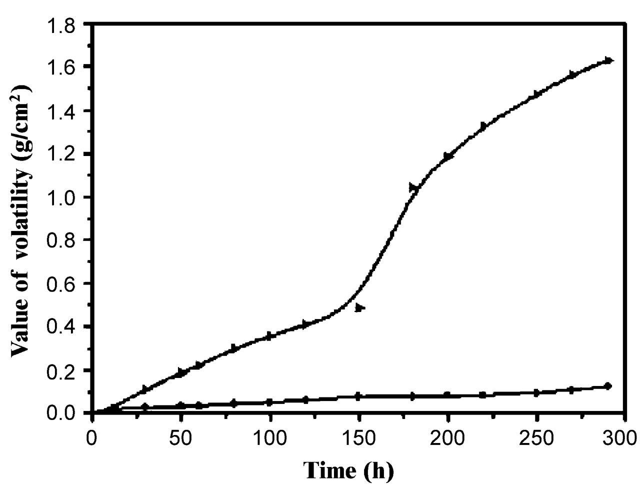

Fig. 1 Volatilities of melts containing Li_2WO_4–B_2O_3 (•) and $K_2Mo_3O_{10}$–B_2O_3 (▶) fluxes

3 Spectroscopic property

Using a spectrometer (Lambda-35, Perkin-Elmer), the transmittance curves in a range from 200 to 500 nm of both crystals with the same thickness of 1.0 mm were measured and are shown in Fig. 2. Here, ultraviolet absorption edge is defined as a wavelength at which the transmission decreases to 1/e of the maximum value of the transmittance curve [14]. For the crystal grown in $K_2Mo_3O_{10}$–B_2O_3 flux, ultraviolet absorption edge is 318 nm. However, ultraviolet absorption edge of the crystal grown in Li_2WO_4–B_2O_3 flux has an ultraviolet-shift of about 40 nm and locates at 278 nm. Therefore, it can be deduced that the defects in the crystal grown in Li_2WO_4–B_2O_3 flux are reduced and the crystal optical quality is improved.

Room temperature σ-polarized absorption spectra of both Yb:YAB crystals in a range from 900 to 1100 nm were recorded with the same spectrometer. The shapes of both

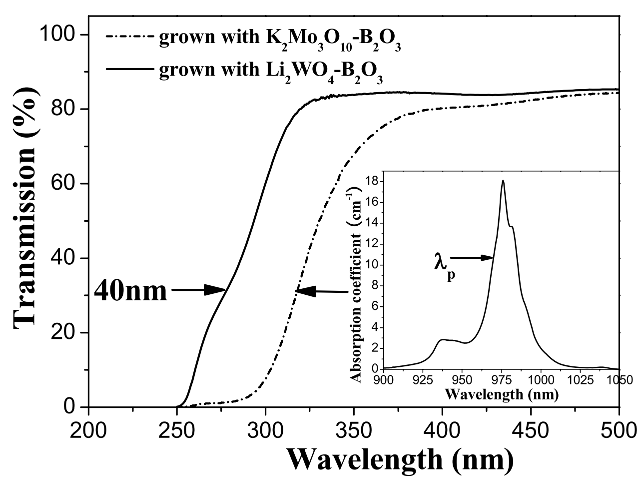

Fig. 2 The transmittance curves in a range from 200 to 500 nm of 1.0-mm thick Yb:YAB crystals grown in Li_2WO_4–B_2O_3 and $K_2Mo_3O_{10}$–B_2O_3 fluxes, respectively. The *inset* shows the room temperature σ-polarized absorption spectra in a range from 900 to 1050 nm of *c*-cut 10 at.% Yb:YAB crystal

spectra are completely identical, which displays the same absorption characteristic of Yb^{3+} ions and then the same crystal field around Yb^{3+} ions for the crystals grown in different fluxes, and shows that the use of different fluxes could not induce the variation of the crystal field around Yb^{3+} ions, such as the appearance of more sites or the increment in lattice disorder. For the sake of brevity, only the spectrum of the crystal grown in Li_2WO_4–B_2O_3 flux is shown in the inset of Fig. 2. The peak absorption coefficient for σ polarization is about 18 cm^{-1} at 976 nm and the full width at half the maximum (FWHM) is 18 nm. Taking the ion density of 5.5×10^{20} cm^{-3} into account, σ-polarized peak absorption cross section at 976 nm was estimated to be 3.27×10^{-20} cm^2. Above spectral parameters are close to those reported previously [1, 4].

Using a microsecond flash lamp (μF900, Edinburgh) as exciting source, fluorescence decay signal at 1040 nm was recorded by a spectrometer (FL920, Edinburgh) when the exciting wavelength was 976 nm and the results are shown in Fig. 3 in a semilog scale. The measured fluorescence lifetimes of $^2F_{5/2}$ multiplet of Yb^{3+} ions were estimated to be about 1.1 and 0.7 ms for Yb:YAB crystals grown in Li_2WO_4–B_2O_3 and $K_2Mo_3O_{10}$–B_2O_3 fluxes, respectively. Because in the measurement the same experimental arrangement was adopted and both samples had the same thickness and Yb^{3+} concentration, the influence of radiation trapping on the measured lifetime for both crystals may be similar [15]. Therefore, although the above measured values deviate from the intrinsic lifetime of Yb:YAB crystal and are longer than those reported previously [1, 4], it is obvious that fluorescence lifetime of the crystal grown in Li_2WO_4–B_2O_3 flux is longer than that grown in $K_2Mo_3O_{10}$–B_2O_3 flux. Furthermore, weaker cooperative upconversion green luminescence was observed by naked eyes in Yb:YAB crystal grown in Li_2WO_4–B_2O_3 flux in the same experimental condition. Above results also reveal the higher optical quality of Yb:YAB crystal grown in Li_2WO_4–B_2O_3 flux, because the longer fluorescence lifetime and weaker upconversion luminescence are mainly originated from the weaker interaction of Yb^{3+} ions with the reduced defects and clusters existing in a crystal [10].

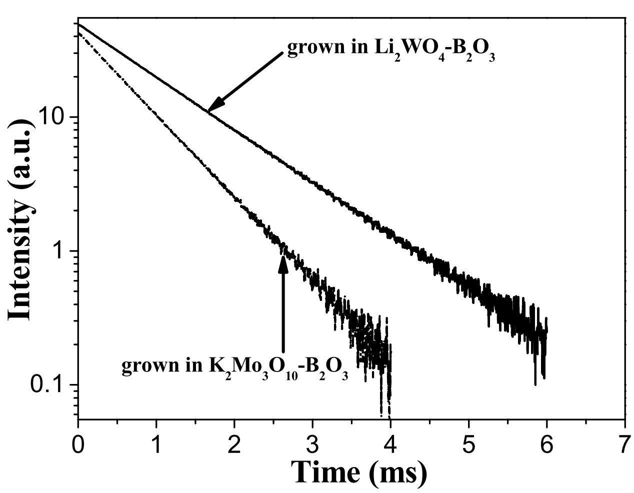

Fig. 3 Fluorescence decay curves at 1040 nm of Yb:YAB crystals grown in Li_2WO_4–B_2O_3 and $K_2Mo_3O_{10}$–B_2O_3 fluxes, respectively. The exciting wavelength is 976 nm

4 Laser property

An end-pumped plano-concave resonator was adopted in laser experiment. A 970 nm fiber-coupled diode laser (800 μm diameter core) from Coherent Inc. was used as pump source. After passing a simple telescopic lens system, pump beam was focused to a spot with waist diameter of about 350 μm in a 1.0-mm thick, *c*-cut sample. The uncoated sample was attached on an aluminum slab with heat-conducting adhesive and there is a hole in the center of the slab for the passing of pump and fundamental laser beams. Because no other device was used to cool the sample, for reducing the influence of pump-induced thermal load on laser performance and avoiding the fracture of sample at high pump power, diode laser was operated in pulse mode. Pump pulse width was 2 ms and duty cycle was 2%. A flat input mirror of the laser cavity had 90% transmission at 970 nm and 99.6% reflectivity around 1040 nm. Three output couplers with a fixed 100 mm radius of curvature (RoC) and different transmissions (0.7%, 1.5%, and 2.9%) around 1040 nm were used in this experiment. In order to reduce cavity loss, the cavity length was set close to RoC of the output couplers. It can be seen from the inset of Fig. 2 that σ-polarized absorption coefficient of the 10 at.% Yb:YAB crystal is about 10.8 cm^{-1} at pump wavelength of 970 nm. Then, about 65% of incident pump power was absorbed by the 1.0-mm thick, *c*-cut sample. The average output power was measured by a laser power meter. Because the duty cycle of quasi-CW laser was 2%, the values in Fig. 4, which were defined as peak output power, were the measured average output powers multiplied by 50.

Figure 4 shows the measured fundamental laser output peak power as a function of absorbed pump peak power for the Yb:YAB crystal grown in Li_2WO_4–B_2O_3 flux. Maximum output peak power of 3.83 W was achieved when absorbed pump peak power was 10.6 W and transmission of output coupler was 2.9%. Absorbed pump threshold was about 2.4 W and slope efficiency η was 58%. When the transmission of output coupler reduced to 0.7%, absorbed pump threshold and slope efficiency decreased to 1.65 W and 35%, respectively. For comparison, laser performance of the Yb:YAB crystal grown in $K_2Mo_3O_{10}$–B_2O_3 flux was also investigated and the case for output coupler transmission of 2.9% is also shown in Fig. 4. Maximum output peak

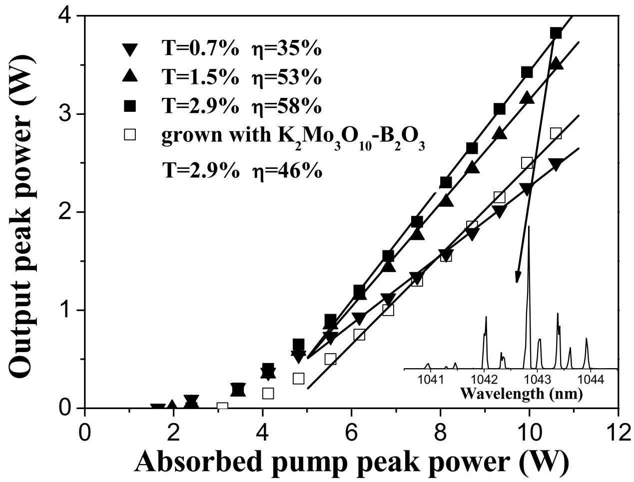

Fig. 4 Output peak power of the Yb:YAB crystal grown in Li_2WO_4–B_2O_3 flux versus absorbed pump peak power at 970 nm for different transmissions T of output couplers. Laser spectrum corresponding to the maximum output peak power and output peak power of the one grown in $K_2Mo_3O_{10}$–B_2O_3 flux for the output coupler with transmission of 2.9% (*open square*) are also shown

power of 2.8 W was achieved when absorbed pump peak power was 10.6 W. Absorbed pump threshold was about 3.1 W and slope efficiency η was 46%. Therefore, in the same experimental condition, higher slope efficiency and lower threshold were realized in the Yb:YAB crystal grown in Li_2WO_4–B_2O_3 flux.

The pump threshold P_{th} of quasi-three-level laser can be expressed as [16, 17]:

$$P_{th} \propto L' + T \qquad (1)$$

where T is the loss due to the output coupling, L' is the loss related to the gain medium and can be written as $L + 2\sigma N_1^0 l$, in which L represents the round-trip loss originating from the scattering at the interface, Fresnel reflection, impurity absorption, and bulk scattering of the gain medium, $2\sigma N_1^0 l$ is the loss due to the population in the lower laser level. Here, σ, N_1^0, and l are the stimulated emission cross section, population in the lower laser level, and thickness of the gain medium, respectively. The loss $2\sigma N_1^0 l$ of the crystal is calculated to be 2.6% when the values $\sigma = 0.8 \times 10^{-20}$ cm^2 [1], $N_1^0 = 1.6 \times 10^{19}$ cm^{-3}, and $l = 0.1$ cm are used. By comparing the laser thresholds for different output coupler transmissions (1.65 W for 0.7%, 1.96 W for 1.5%, and 2.4 W for 2.9%), the loss L' of the crystal grown in Li_2WO_4–B_2O_3 flux can be estimated to be about 4.2%. Then, the round-trip loss L of the crystal grown in Li_2WO_4–B_2O_3 flux is about 1.6%. Considering the crystal thickness l of 0.1 cm, the internal loss coefficient $\delta = L/(2l)$ of the crystal is calculated to be 0.08 cm^{-1}. By the same method, the loss coefficient δ of the crystal grown in $K_2Mo_3O_{10}$–B_2O_3 flux is about 0.1 cm^{-1} and the value of Yb:YAB crystal used in Ref. [4] is calculated to be 0.11 cm^{-1} from the reported absorbed pump threshold at different output coupler transmissions [4].

Laser spectra of both Yb:YAB crystals were recorded with a monochromator (Triax550, Jobin-Yvon) associated with a TE-cooled Ge detector (DSS-G025T, Jobin-Yvon). Because of the similarity of the spectra for both crystals at various absorbed pump powers and output coupler transmissions, only laser spectrum of the Yb:YAB crystal grown in Li_2WO_4–B_2O_3 flux with output coupler transmission of 2.9% and absorbed pump peak power of 10.6 W is shown in the inset of Fig. 4 for the sake of brevity. The wavelength of output laser is in a range from 1041 to 1044 nm and centered at 1043 nm. Output laser beams were unpolarized and the ratios of output powers of Yb^{3+}:YAB crystal between horizontal and vertical polarizations were measured to be close to unity for all output coupler transmissions and in the range of absorbed pump powers.

5 Conclusions

A 10 at.% Yb:YAB crystal with higher optical quality has been grown successfully in Li_2WO_4–B_2O_3 flux. The absorption characteristics of Yb^{3+} ions in the crystals grown in Li_2WO_4–B_2O_3 and $K_2Mo_3O_{10}$–B_2O_3 fluxes are the same. However, shorter ultraviolet absorption edge and longer fluorescence lifetime of Yb^{3+} ions were observed in the crystal grown in Li_2WO_4–B_2O_3 flux due to the reduction of defects in the crystal. Furthermore, laser at 1043 nm with higher slope efficiency of 58% and lower threshold of 2.4 W were also realized for the crystal grown in Li_2WO_4–B_2O_3 flux; whereas slope efficiency and threshold for the one grown in $K_2Mo_3O_{10}$–B_2O_3 flux were 46% and 3.1 W, respectively, in the same experimental condition. Consequently, the Yb:YAB crystal grown in Li_2WO_4–B_2O_3 flux may be a more appropriate gain medium for solid-state lasers, including microchip and SFD green lasers.

Due to the limit of diode laser, the pump wavelength could only be set at 970 nm in this work rather than the peak absorption wavelength of the Yb:YAB crystal at 976 nm. For σ polarization, absorption coefficient at 976 nm is 18 cm^{-1} and much larger than the 10.8 cm^{-1} at 970 nm (see the inset of Fig. 2). When pump wavelength is tuned to 976 nm, a thinner Yb:YAB crystal can be used in the experiment for keeping the same absorption of the incident pump light. Consequently, the round-trip loss of the crystal originated from the defects will be reduced. Then, lower threshold and higher slope efficiency may be realized in the Yb:YAB laser. The main aim of this work is to investigate the effect of different fluxes used in the growth process on the crystal optical quality. Therefore, although only quasi-CW laser experiment was carried out in this work and the obtained slope efficiency was still lower than that (72%) in the Yb:YAB crystal grown in the complex polymolybdate flux [4], the improvement of laser performance obtained in the same experimental condition for the crystal grown in Li_2WO_4–B_2O_3 flux has been demonstrated. It can be expected that when the Yb:YAB crystal grown in Li_2WO_4–B_2O_3 flux is used in the same experimental condition reported in Ref. [4], a slope efficiency closer to the theoretical limit (about 90%) may be obtained.

Acknowledgements This work has been supported by the National Natural Science Foundation of China (grants 50802094) and the Knowledge Innovation Program of the Chinese Academy of Sciences (grant 48808318-7).

References

1. P. Wang, J.M. Dawes, P. Dekker, D.S. Knowles, J.A. Piper, B. Lu, J. Opt. Soc. Am. B **16**, 63 (1999)
2. S. Rivier, U. Griebner, V. Petrov, H. Zhang, J. Li, J. Wang, J. Liu, Appl. Phys. B **93**, 753 (2008)
3. P.A. Burns, J.M. Dawes, P. Dekker, J.A. Piper, J. Li, J. Wang, Opt. Commun. **207**, 315 (2002)
4. J. Liu, X. Mateos, H. Zhang, J. Li, J. Wang, V. Petrov, IEEE J. Quantum Electron. **43**, 385 (2007)
5. P. Dekker, J.M. Dawes, J.A. Piper, Y. Liu, J. Wang, Opt. Commun. **195**, 431 (2001)
6. P. Dekker, J.M. Dawes, J.A. Piper, J. Opt. Soc. Am. B **22**, 378 (2005)
7. D. Jaque, J.C. Lagomacini, C. Jacinto, T. Catunda, Appl. Phys. Lett. **89**, 121101 (2006)
8. A. Pugzlys, G. Andriukaitis, D. Sidorov, A. Irshad, A. Baltuska, W.J. Lai, P.B. Phua, L. Su, J. Xu, H. Li, R. Li, S. Alisauskas, A. Marcinkevicius, M.E. Fermann, L. Giniunas, R. Danielius, Appl. Phys. B **97**, 339 (2009)
9. N.I. Leonyuk, L.I. Leonyuk, Prog. Cryst. Growth Charact. **31**, 179 (1995)
10. I. Foldvari, E. Beregi, A. Baraldi, R. Capelletti, W. Ryba-Romanowski, G. Dominiak-Dzik, A. Munoz, R. Sosa, J. Lumin. **102–103**, 395 (2003)
11. J. Li, G. Xu, S. Han, J. Fan, J. Wang, J. Cryst. Growth **311**, 4251 (2009)
12. A. Peter, K. Polgar, E. Beregi, J. Cryst. Growth **209**, 102 (2000)
13. P. Dekker, J.M. Dawes, Appl. Phys. B **83**, 267 (2006)
14. I.G. Kim, S. Takekawa, Y. Furukawa, M. Lee, K. Kitamura, J. Cryst. Growth **229**, 243 (2001)
15. D.S. Sumida, T.Y. Fan, Opt. Lett. **19**, 1343 (1994)
16. T.Y. Fan, R.L. Byer, IEEE J. Quantum Electron. **QE-23**, 605 (1987)
17. W.P. Risk, J. Opt. Soc. Am. B **5**, 1412 (1988)